

An Enzymatic TMPRSS2 Assay for Assessment of Clinical Candidates and Discovery of Inhibitors as Potential Treatment of COVID-19

Jonathan H. Shrimp¹, Stephen C. Kales¹, Philip E. Sanderson¹, Anton Simeonov¹, Min Shen¹, Matthew D. Hall^{1,2}

¹National Center for Advancing Translational Sciences, National Institutes of Health, Rockville, MD, 20850

²Correspondence to: Matthew D. Hall (hallma@mail.nih.gov)

Abstract

SARS-CoV-2 is the viral pathogen causing the COVID19 global pandemic.

Consequently, much research has gone into the development of pre-clinical assays for the discovery of new or repurposing of FDA-approved therapies. Preventing viral entry into a host cell would be an effective antiviral strategy. One mechanism for SARS-CoV-2 entry occurs when the spike protein on the surface of SARS-CoV-2 binds to an ACE2 receptor followed by cleavage at two cut sites (“priming”) that causes a conformational change allowing for viral and host membrane fusion. This fusion event is preceded by release of viral RNA within the host cell. TMPRSS2 has an extracellular protease domain capable of cleaving the spike protein to initiate membrane fusion. Additionally, knock-out studies in mice have demonstrated reduced infection in the absence of TMPRSS2 with no detectable physiological impact; thus, TMPRSS2 is an attractive target for therapeutic development. A validated inhibitor of TMPRSS2 protease activity would be a valuable tool for studying the impact TMPRSS2 has in viral entry and potentially be an effective antiviral therapeutic. To enable inhibitor discovery and profiling of FDA-approved therapeutics, we describe an assay for the biochemical screening of recombinant TMPRSS2 suitable for high throughput application. We demonstrate effectiveness to quantify inhibition down to subnanomolar concentrations by assessing the inhibition of camostat, nafamostat and gabexate, clinically approved agents in Japan for pancreatitis due to their inhibition of trypsin-like proteases.

Nafamostat and camostat are currently in clinical trials against COVID19. The rank order potency for the three inhibitors is: nafamostat ($IC_{50} = 0.27$ nM), camostat ($IC_{50} =$

6.2 nM) and gabexate ($IC_{50} = 130$ nM). Further profiling of these three inhibitors against a panel of proteases provides insight into selectivity and potency.

Introduction

The SARS-CoV-2 pandemic has driven the urgent need to rapidly identify therapeutics for both preventing and treating infected patients. Given that no approved therapeutics for treating any coronaviruses existed at the time SARS-CoV-2 emerged (late 2019), early attention has focused on drug repurposing opportunities^{1, 2}. Drug repurposing is an attractive approach to treating SARS-CoV-2, as active drugs approved for use in humans in the United States or by other regulatory agencies, or unapproved drug candidates shown to be safe in human clinical trials, can be nominated for fast-track to the clinic. For example, remdesivir (GS-5734, Gilead Sciences Inc.), is an inhibitor of viral RNA-dependent RNA polymerase that had previously been in clinical trials for treating Ebola virus. Remdesivir was rapidly shown to be active against SARS-CoV-2 *in vitro* and in clinical trials, which resulted in the FDA granting emergency use authorization and full approval in Japan³. The delineation of targets and cellular processes that mediate SARS-CoV-2 infection and replication forms the basis for the development of assays for drug repurposing screening and subsequent full-fledged therapeutic development programs.

One therapeutic target receiving significant attention is the human host cell transmembrane protease serine 2 (TMPRSS2, Uniprot – O15393⁴). TMPRSS2 is anchored to the extracellular surface of the cell, where it exerts its enzymatic activity. While its precise physiologic substrate is not clear, TMPRSS2 gene fusions are common in prostate cancer, resulting in its overexpression⁴. The SARS-CoV-2 virus enters cells *via* its spike protein first binding to the cell-surface enzyme ACE2, and

evidence suggests that TMPRSS2 then proteolytically cleaves a sequence on the spike protein, facilitating a conformation change that ‘primes’ it for cell entry (Figure 1A).

TMPRSS2 was first shown to facilitate viral entry of the coronaviruses SARS-CoV and HCoV-NL63 in cells engineered to overexpress TMPRSS2, and by inhibition with the trypsin-like serine protease inhibitor, camostat⁵. When the MERS-CoV outbreak occurred, TMPRSS2-overexpressing cells were again shown to facilitate cell infection, TMPRSS2 was shown to degrade the MERS-CoV spike protein, and camostat was shown to limit cell entry⁶. The structurally related trypsin-like serine protease inhibitor nafamostat was shown to similarly inhibit spike protein-mediated cell fusion of MERS-CoV⁷. Given the strong evidence that TMPRSS2 mediates coronavirus entry, when SARS-CoV-2 emerged it was soon demonstrated through loss- and gain-of-function experiments that TMPRSS2 is retained as a mediator of cell infection, and that this can be inhibited by camostat⁸.

Camostat (also called FOY-305) is a trypsin-like serine protease inhibitor approved in Japan (as the mesylate salt) for the treatment of pancreatitis and reflux esophagitis⁹. Given its status as an approved agent that is orally administered, safe and well tolerated in humans, and can inhibit cellular entry, camostat mesylate received attention as a drug repurposing candidate. At least six clinical trials for treating patients are currently underway¹⁰. However, while indirect evidence exists that camostat and related compounds inhibit TMPRSS2-mediated cell entry of SARS-CoV-2, no direct biochemical evidence exists in the literature. Camostat was developed by Ono Pharmaceuticals (patented in 1977^{9, 11}). While a specific report of its development does

not appear to be published, it is a highly potent inhibitor of trypsin¹² ($IC_{50} \approx 50$ nM), and it cross-inhibits other proteases. Two other structurally related inhibitors, nafamostat and gabexate (FOY-307), are also approved in Japan for treating pancreatitis and show potential for activity against SARS-CoV-2, and trials with nafamostat have also been reported. While TMPRSS2 biochemical assays have been reported for understanding its role in prostate cancer^{13, 14}, the three inhibitors have not been demonstrated to inhibit TMPRSS2 and the rank potency of the inhibitors against TMPRSS2 is not known.

In response to the COVID19 public health emergency, we are developing both protein/biochemical and cell-based assays to interrogate several biological targets to enable identification of potential therapeutic leads. Our initial focus is on performing drug repurposing screening for each assay and rapidly sharing the data through the NCATS OpenData portal for COVID19¹⁵. As part of this effort, we sought to develop a biochemical assay for measuring the activity of TMPRSS2 to enable the evaluation of existing drug repurposing candidates and to enable drug repurposing screening.

Herein we report the development of a TMPRSS2 fluorogenic biochemical assay and testing of clinical repurposing candidates for COVID19. Activity of TMPRSS2 constructs, and assessment of a number of substrates was first performed. The best substrate was then used to assess enzyme kinetics and establish a K_m value for the substrate, to define assay conditions and demonstrate suitability of the assay in 384- and 1536-well plates. The inhibitors camostat, nafamostat and gabexate were assessed. To

understand their relative activities, we also profiled them against a panel of human proteases.

Methods

Reagents

Recombinant Human TMPRSS2 protein (human TMPRSS2 residues 106-492, N-terminal 6x His-tag) (Cat # TMPRSS2-1856H) was acquired from Creative BioMart (Shirley, NY). Peptides obtained from Bachem include: Boc-Leu-Gly-Arg-AMC . acetate (Cat#: I-1105), Boc-Gln-Ala-Arg-AMC . HCl (Cat#: I-1550), Ac-Val-Arg-Pro-Arg-AMC . TFA (Cat#: I-1965), Cbz-Gly-Gly-Arg-AMC . HCl (Cat#: I-1140). Peptides custom ordered from LifeTein (Somerset, NJ) include: Cbz-D-Arg-Gly-Arg-AMC, Cbz-D-Arg-Pro-Arg-AMC.

Fluorogenic Peptide Screening Protocol – 384-well plate

To a 384-well black plate (Greiner 781900) was added Boc-Gln-Ala-Arg-AMC (62.5 nL) and inhibitor (62.5 nL) using an ECHO 655 acoustic dispenser (LabCyte). To that was added TMPRSS2 (750 nL) in assay buffer (50 mM Tris pH 8, 150 mM NaCl) to give total reaction volume of 25 μ L. Following 1 hr incubation at RT, detection was done using the PHERAstar with excitation: 340 nm and emission: 440 nm.

Fluorescence counter assay – 384-well plate

To a 384-well black plate (Greiner 781900) was added 7-amino-methylcoumarin (62.5 nL) and inhibitor or DMSO (62.5 nL) using an ECHO 655 acoustic dispenser (LabCyte). To that was added assay buffer (50 mM Tris pH 8, 150 mM NaCl) to give total reaction volume of 25 μ L. Detection was done using the PHERAstar with excitation: 340 nm and emission: 440 nm. Fluorescence was normalized relative to a negative control containing DMSO-only wells (0% activity, low fluorescence) and a positive control containing AMC only (100% activity, high fluorescence). An inhibitor causing

fluorescence quenching would be identified as having a concentration-dependent decrease on AMC fluorescence.

Fluorogenic Peptide Screening Protocol – 1536-well plate

To a 1536-well black plate was added Boc-Gln-Ala-Arg-AMC substrate (20 nL) and inhibitor (20 nL) using an ECHO 655 acoustic dispenser (LabCyte). To that was dispensed TMPRSS2 (150 nL) in assay buffer (50 mM Tris pH 8, 150 mM NaCl) using a BioRAPTR (Beckman Coulter) to give total reaction volume of 5 μ L. Following 1 hr incubation at RT detection was done using the PHERAstar with excitation: 340 nm and emission: 440 nm.

TMPRSS2 Assay Protocol

The TMPRSS2 biochemical assay was performed according to the assay protocol shown in Table 1.

Table 1. Detailed TMPRSS2 biochemical protocol.

Step #	Process	Notes
1	20 nL of peptide substrate dispensed into 1536-well plates.	Peptide (dissolved in DMSO) dispensing performed using an ECHO 655 acoustic dispenser (LabCyte). Corning® 1536-well Black Polystyrene, square well, high base, non-sterile, non-treated; Cat #3724
2	20 nL of inhibitor or vehicle control (DMSO) dispensed into 1536-well plates.	Inhibitor or vehicle control (DMSO) dispensing performed using an ECHO 655 acoustic dispenser (LabCyte).
3	TMPRSS2 diluted in assay buffer dispensed into 1536-well plates.	TMPRSS2 (33.5 μ M, 150 nL) in assay buffer (50 mM Tris pH 8, 150 mM NaCl) dispensing performed using a BioRAPTR (Beckman Coulter). Total reaction volume of 5 μ L.
4	Incubate at RT for 1 hr at RT	Final assay conditions are 10 μ M peptide and 1 μ M TMPRSS2 in assay

		buffer (50 mM Tris-HCl, pH 8, 150 mM NaCl)
5	Read on PHERAstar FSX (BMG Labtech)	Fastest read settings, Fluorescence Intensity module, 340 nm excitation, 440 nm emission) (Cat # 1601A2, BMG Labtech)

Data Process and Analysis

To determine compound activity in the assay, the concentration-response data for each sample was plotted and modeled by a four-parameter logistic fit yielding IC₅₀ and efficacy (maximal response) values. Raw plate reads for each titration point were first normalized relative to a positive control containing no enzyme (0% activity, full inhibition) and a negative control containing DMSO-only wells (100% activity, basal activity). Data normalization, visualization and curve fitting were performed using Prism (GraphPad, San Diego, CA).

Results

To identify inhibitors of TMPRSS2 that may be used to validate its role in SARS-CoV-2 entry and potentially expedite to clinical trials, we developed a biochemical assay using active TMPRSS2 protease and a fluorogenic peptide substrate (Figure 1B). Initially, we screened six candidate fluorogenic peptide substrates, Boc-Gln-Ala-Arg-AMC¹⁴, Cbz-D-Arg-Gly-Arg-AMC¹³, Cbz-D-Arg-Pro-Arg-AMC¹³, Boc-Leu-Gly-Arg-AMC^{13, 16}, Cbz-Gly-Gly-Arg-AMC^{13, 17} and Ac-Val-Arg-Pro-Arg-AMC, most of which had been demonstrated within the literature to be cleaved by TMPRSS2. Each peptide contains a 7-amino-4-methylcoumarin (AMC) fluorophore that is liberated following enzymatic cleavage.

Candidate substrates were tested to both confirm that the TMPRSS2 construct was biochemically active (other commercial constructs sourced and tested were not active, data not shown), and to identify the most cleavable substrate, indicated by the greatest production of fluorescence from the fluorogenic product AMC (Figure 2A). The peptide Boc-Gln-Ala-Arg-AMC had a 27% conversion at 60 min, which was the highest conversion observed, and was used for further assay optimization and inhibitor screening with the recombinant TMPRSS2 protein from Creative BioMart (Figure 1C).

Next, a TMPRSS2 titration was performed at constant substrate concentration (25 μ M) to identify an appropriate enzyme concentration that achieves ~20% substrate conversion in 60 min, and this was found to be 1 μ M (Figure 2B). We then varied assay buffer conditions, such as Tris-HCl buffer pH, DMSO and Tween20 concentrations to further optimize enzymatic activity and determine tolerance to DMSO and Tween20 that are required for inhibitor screening. Noticing that trypsin activity is optimal at pH 7.5 –

8.5¹⁸, we tested a few different pH > 7 and demonstrated that pH of 9 had highest % conversion (Figure 2C). However, a pH of 8, which had nearly identical % conversion, was chosen to proceed for further assay optimization and inhibitor screening. Next, enzymatic activity was shown to be tolerant of Tween20 at 0.01% (data not shown), and DMSO up to 4% (data not shown), well above the DMSO concentrations of <1% v/v typically applied during the testing of inhibitors.

Finally, using our optimized assay buffer conditions, we determined the K_m of our peptide substrate to be 33 μ M (Figure 2D). The concentration of substrate selected for the biochemical assay was set below K_m at 10 μ M to ensure susceptibility to competitive inhibitors (detailed protocol provided in Table 1). Positive and negative control conditions were assessed in 384- and 1536-well plate formats to determine a signal:background (S:B) and a Z' appropriate for HTS. The S:B and Z' in a 384-well plate were 3.6 and 0.86, respectively (Figure 2E), and in a 1536-well plate the S:B and Z' were 3.2 and 0.86, respectively (Figure 2F). These data demonstrate appropriate performance for this assay within both plate formats to be useful for HTS (Figure 2F).

Next, using the established assay in 384-well format, we tested the inhibition of TMPRSS2 by camostat, nafamostat and gabexate (Figure 3). These three compounds are trypsin-like serine protease inhibitors clinically approved in Japan that have recently been demonstrated to inhibit SARS-CoV-2 infection in the lung-derived human cell line Calu-3¹⁹, but direct inhibition of TMPRSS2 biochemical activity has not previously been demonstrated. We found that nafamostat (currently in clinical trials) (IC_{50} = 0.27 nM) is

the most potent among the three inhibitors, while camostat (currently in clinical trials) shows low nM potency ($IC_{50} = 6.2$ nM). Gabexate was significantly less potent ($IC_{50} = 130$ nM). To ensure these inhibitors are not false-positive artifacts of the assay by quenching the fluorescence of the cleaved AMC, a counter-assay to detect quenching of AMC was performed. The counter assay involved addition of inhibitors in various concentrations to AMC held at 1 μ M, which approximates a 10% conversion from the enzymatic cleavage. The counter assay demonstrated that these inhibitors had no dose-response effects on the fluorescence from AMC, indicating there was no quenching of AMC fluorescence from the inhibitors tested (overlaid data, Figure 3a-c). This data supports the conclusions drawn in cell-based studies that the ability of camostat and nafamostat to inhibit cell entry of virus is caused by direct inhibition of TMPRSS2 (though inhibition of other proteases may contribute to cellular activity observed, *vide infra*).

To assess potential activity against other physiologically relevant proteases, camostat, nafamostat and gabexate were profiled against a panel of human recombinant protease assays, spanning multiple enzyme families and classes in 10-point concentration response (RB; Figure 4). Consistent with their similar chemical structures and defined activity as trypsin-like serine protease inhibitors²⁰, inhibition patterns were similar among the three inhibitors tested, demonstrating concentration-response inhibition of several trypsin-like serine proteases, including members of the trypsin family (trypsin, kallikreins). All three inhibitors also demonstrated potent activity towards the plasma trypsin-like proteases, plasmin and FXIa, as well as Matriptase 2 (a.k.a. TMPRSS6), a

member of the type II transmembrane protease family which includes TMPRSS2²¹. Nafamostat again demonstrated the most potent inhibitory activity, followed by camostat, with gabexate demonstrating the lowest potency. Of the proteases tested, only Kallikrein 12 demonstrated greater sensitivity to gabexate relative to nafamostat and camostat. Dose-response data revealed no inhibitory activity against several matrix metalloproteases (MMP), caspases, and only modest activity against the cysteine protease, Cathepsin S.

Additional profiling of 40+ human proteases at single concentration using 10 μ M (BPS Biosciences; Supplementary Figure 1) confirmed sensitivity observed by Matriptase 2 and several kallikreins, with highest inhibitory activity against another plasma trypsin-like serine protease, APC, which plays a critical role in coagulation²². This diverse panel also included several caspases and ubiquitin specific proteases (USP), all of which demonstrated little to no sensitivity to either inhibitor. The conserved rank order demonstrated here against numerous proteases tested suggests that neither compound conveys improved target selectivity but rather improved potency, which highlights the need for novel, more specific inhibitors of TMPRSS2.

Discussion

We developed a fluorogenic biochemical assay for measuring recombinant human TMPRSS2 activity for high-throughput screening that can be readily replicated and used to demonstrate that nafamostat is a more potent inhibitor than camostat and gabexate. The fluorogenic assay approach taken here has advantages and disadvantages. The assay performs well and was readily scaled to 1536-well format for potential high-throughput robotic screening, can be monitored in real-time, and activity is easily detected by the liberation of a fluorophore. The substrate was selected based on the maximal activity of TMPRSS2 against it compared with other substrate candidates, and can be considered a tool substrate, rather than one that is physiologically relevant in the context of the action of TMPRSS2 against its SARS-CoV-2 spike protein cleavage site. A disadvantage that is common to all fluorescence-based assay readouts is the potential for inhibitory compounds from screening to be false-positive artifacts, by quenching the fluorescence of the AMC product, but a simple counter-assay for AMC quenchers can be used to identify false-positives. This counter assay was done on those inhibitors profiled here to demonstrate there was no dose-response quenching of AMC fluorescence (overlaid data, Figure 3a-c).

Two other reports of biochemical assays for TMPRSS2 exist, though their study was unrelated to the role of TMPRSS2 in SARS-CoV-2 entry. Lucas *et al.* examined TMPRSS2 in the context of prostate cancer. They reported a HTS screen at a single concentration, producing several screening hits including the FDA-approved bromhexine hydrochloride¹⁴ (BHH) and BHH has also been discussed as a potential

drug repurposing TMPRSS2 inhibitor candidate²³. Unfortunately, no details of the assay utilized, scale of assay, or its development were described, but the substrate identified in our study as the most amenable for HTS (Boc-Gln-Ala-Arg-AMC) was also used in the Lucas study. Meyer *et al.* examined several peptide AMC substrates for TMPRSS2 and used a biochemical assay to assess modified peptide substrates as TMPRSS2 inhibitors, some with observed inhibition constants of approximately 20 nM¹³. They found a high correlation between inhibition constants of inhibitors between TMPRSS2 and matriptase, similar to the cross-inhibition seen from the three inhibitors profiled within our assay. Additionally, they report a low active TMPRSS2 concentration in the enzyme stock solution. In our study, the enzyme concentration used was 1 μ M based on the manufacturer's supplied concentration, but we do not know the proportion of enzyme that is active, and the concentration of active enzyme may be far lower than total enzyme present.

We report here for the first time the direct biochemical inhibition of TMPRSS2 by three clinical agents of interest in COVID19. Given the clinical trial attention on camostat and nafamostat for treating COVID19, our finding that nafamostat demonstrates greater potency against TMPRSS2 supports its evaluation in clinical trials. Protease profiling revealed activity against a range of trypsin-like serine proteases (and greater potency than against TMPRSS2), but activity was restricted to this protease class and compounds did not generally inhibit other protease classes such as matrix metalloproteases (MMPs), caspases, and ubiquitin-specific proteases (USPs). Camostat and nafamostat development was reported to focus on trypsin, plasmin, and

kallikrein^{12, 24}, because of the role these targets played in pancreatitis, reflux esophagitis & hyperproteolytic conditions, and activity against these enzymes was certainly observed in the protease panel.

Beyond the evaluation of current inhibitors, we demonstrated acceptable reproducibility and S:B indicating its suitability in a drug repurposing screen to support the development of new inhibitors of TMPRSS2. There are several reasons why a new clinical candidate may be valuable. A number of coronaviruses have been shown to rely on TMPRSS2 for cellular entry (described in the introduction), so a potent, orally available TMPRSS2 inhibitor could be invaluable as a repurposing candidate for treating future emergent coronaviruses. COVID19 is associated with acute respiratory distress syndrome (ARDS). The lung pathology of the ARDS shows microvascular thrombosis and hemorrhage, and has been characterized as disseminated intravascular coagulation (DIC) with enhanced fibrinolysis, or as diffuse pulmonary intravascular coagulopathy^{25, 26}. This coagulopathy can lead to pulmonary hypertension and cardiac injury. Trypsin-like serine proteases are involved in SARS-CoV-2 cell entry (TMPRSS2), in the coagulation cascade (APC) and in the enhanced fibrinolysis (plasmin). As shown here, camostat, nafamostat and gabexate directly inhibit enzymes involved in all these processes. Clinical development of this class of compounds could thus be directed towards treatment of the infection through inhibition of viral entry, towards treatment of the coagulopathy, or conceivably, both. However, the strategies used to treat viral infection and coagulopathies are very different. The former aims to achieve maximum viral suppression, with dose limited by safety and tolerability. The latter seeks to strike

the delicate balance between suppression of thrombosis while managing the inevitable increased risk of bleeding. For this reason, the known clinical trials planned or underway for nafamostat and camostat can be divided into three categories: those whose primary endpoint is focused on limiting or preventing infection, those whose primary endpoint is focused on management of ARDS and advanced disease, and those which may capture treatment benefit through either mechanism.

Nafamostat is approved and marketed in Japan and S. Korea and is typically prescribed to treat acute symptoms of pancreatitis and to treat DIC. It is administered by IV infusion and has a plasma half-life ($t_{1/2}$) of about 23 min²⁷. Clinical trials to test the hypothesis that nafamostat can lower lung function deterioration and need for intensive care admission in COVID-19 patients, and that nafamostat can improve the clinical status of COVID-19 patients with pneumonia have been registered. Camostat is approved in Japan for the treatment acute symptoms of chronic pancreatitis and postoperative reflux esophagitis²⁸. The treatment regimen is typically 200 mg PO, every eight hours.

Camostat is a pro-drug as the parent drug is not detected in plasma. The terminal ester is rapidly hydrolysed in plasma ($t_{1/2} < 1$ min) to 4-(4-guanidinobenzoyloxy)phenylacetic acid (FOY-251) which has a mean terminal half-life = 1 h²⁹. FOY-251 and camostat are reported to have similar activities against trypsin, thrombin, plasma kallikrein and plasmin¹², but the activity of FOY-251 against TMPRSS2 remains to be determined.

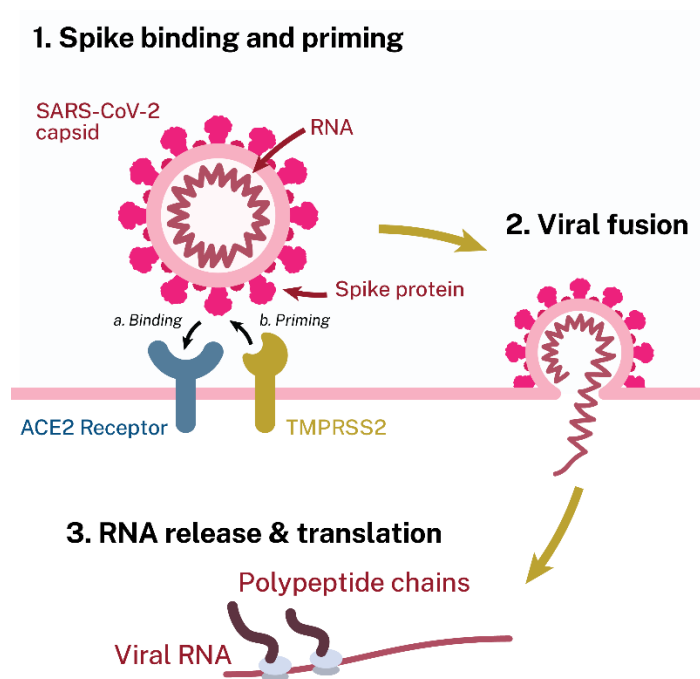
There are six registered clinical trials studying camostat, of which only one is focused on coagulopathy. The other trials are focused on early, mild or moderate disease.

Gabexate is an IV drug approved for marketing in Italy and Japan was shown to be effective in treating patients with sepsis-associated disseminated intravascular

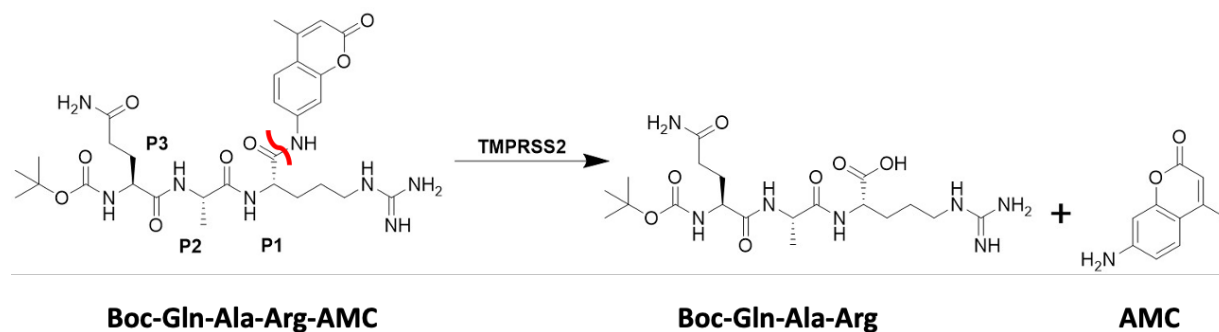
coagulation and treating acute pancreatitis. It is clearly much less potent than nafamostat and there are no registered COVID-19 clinical studies with it. In summary, of the three drugs in the class, nafamostat is being studied as the preferred drug in an ICU setting as it can be titrated against coagulation markers as a treatment for coagulopathy, while considering its antiviral effect as a bonus. In outpatient, early diagnosis, or prophylactic settings, camostat is being studied predominantly with the primary purpose as an antiviral. In these latter settings there is room for new, selective TMPRSS2 inhibitors which could achieve higher levels of inhibition without incurring a bleeding risk.

The biochemical TMPRSS2 assay we disseminate here is a simple, and HTS-amenable approach to TMPRSS2 inhibitor therapeutic development. Clinical trials of nafamostat for COVID19 have been reported, and we believe it warrants evaluation given its superior activity over camostat, as demonstrated herein.

(A)



(B)



(C)

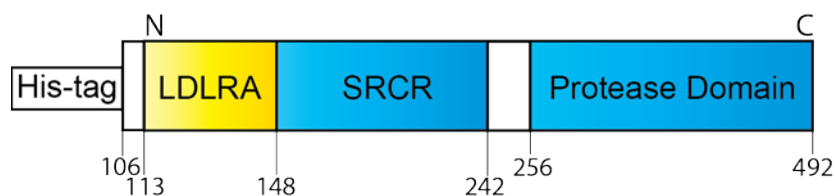
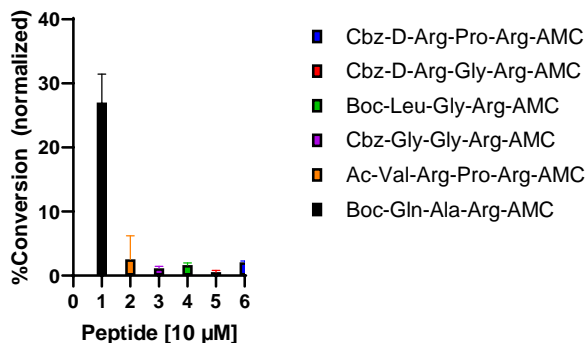


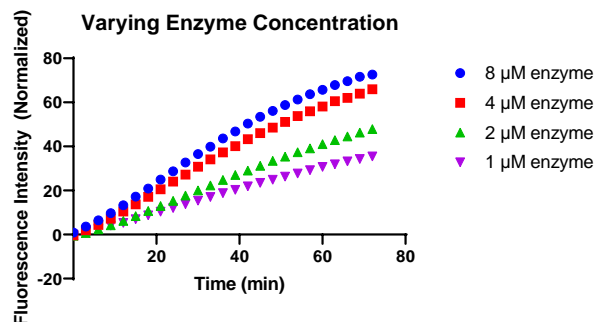
Figure 1: A) Scheme demonstrating the role TMPRSS2 plays in priming SARS-CoV-2 for cellular entry. Spike protein first binds to ACE2 ('Binding'), followed by proteolytic action of TMPRSS2 ('Priming') prior to viral fusion. **B)** Scheme displaying the enzymatic

assay principle. The fluorogenic peptide substrate Boc-Gln-Ala-Arg-AMC has low fluorescence compared to the fluorescent 7-amino-4-methylcoumarin (AMC), which is liberated upon proteolytic cleavage. The scissile bond is indicated in red. **C**) Schematic of the truncated TMPRSS2 recombinant protein, containing the low-density lipoprotein receptor A (LDLRA) domain, scavenger receptor cysteine-rich (SRCR) domain and protease domain utilized in the biochemical assay.

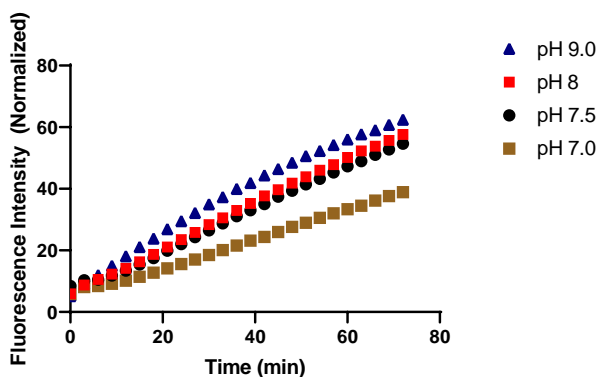
A



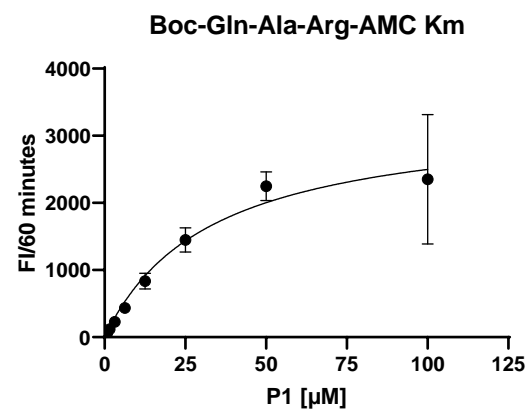
B



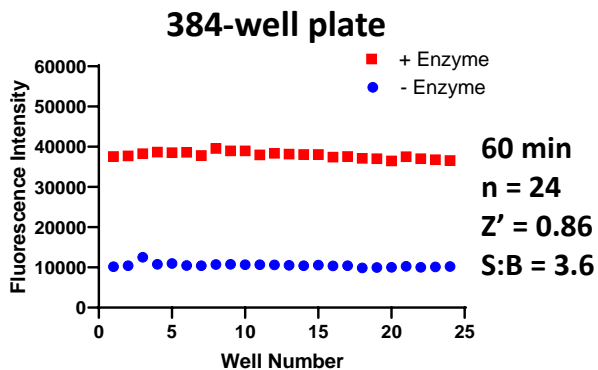
C



D



E



F

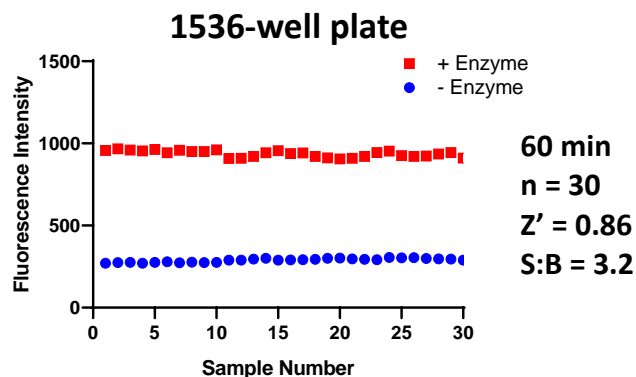
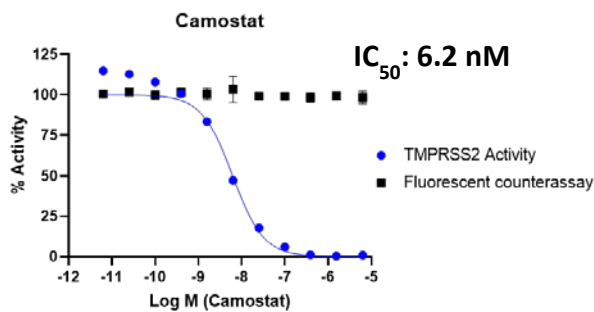
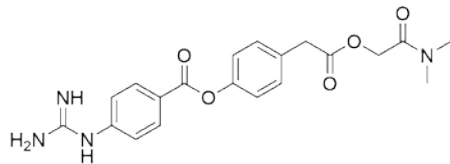
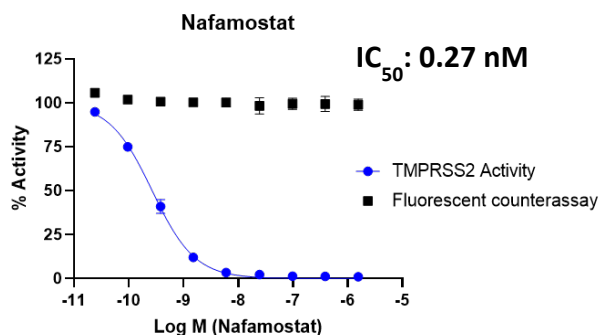
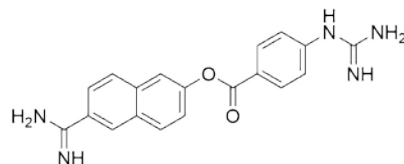


Figure 2: Assessment of enzymatic activity and optimization of TMPRSS2 biochemical assay. **A)** Various AMC-labeled peptides. Peptide [10 μ M], TMPRSS2 [1 μ M] in Tris-HCl pH8. **B)** TMPRSS2 titration using Boc-Gln-Ala-Arg-AMC peptide [25 μ M] in Tris-HCl pH8. **C)** Varying Tris-HCl buffer pH. TMPRSS2 [4 μ M], Boc-Gln-Ala-Arg-AMC [25 μ M]. **D)** K_m of Boc-Gln-Ala-Arg-AMC while TMPRSS2 [1 μ M], Tris-HCl pH8. **E)** 384-well plate S:B and Z'. TMPRSS2 [1 μ M], Boc-Gln-Ala-Arg-AMC [10 μ M], Tris-HCl pH8. **F)** 1536-well plate S:B and Z'. TMPRSS2 [1 μ M], Boc-Gln-Ala-Arg-AMC [10 μ M], Tris-HCl pH8.

A



B



C

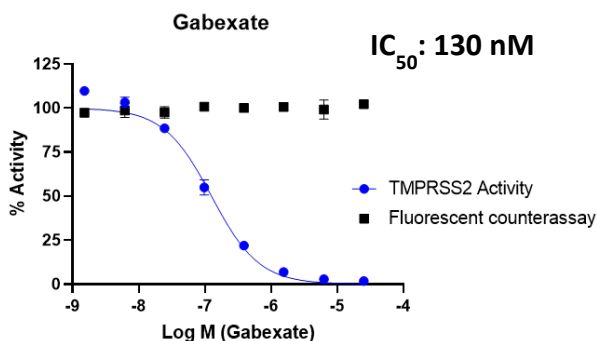
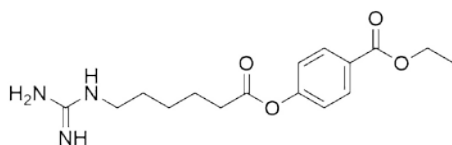


Figure 3: Activity of clinically approved inhibitors against TMPRSS2 (blue), and fluorescent counter-assay (black). The molecular structures and dose-response inhibition of TMPRSS2 by **A)** camostat, **B)** nafamostat, and **C)** gabexate are shown. The calculated concentrations required for 50% inhibition (IC_{50}) are displayed in nM.

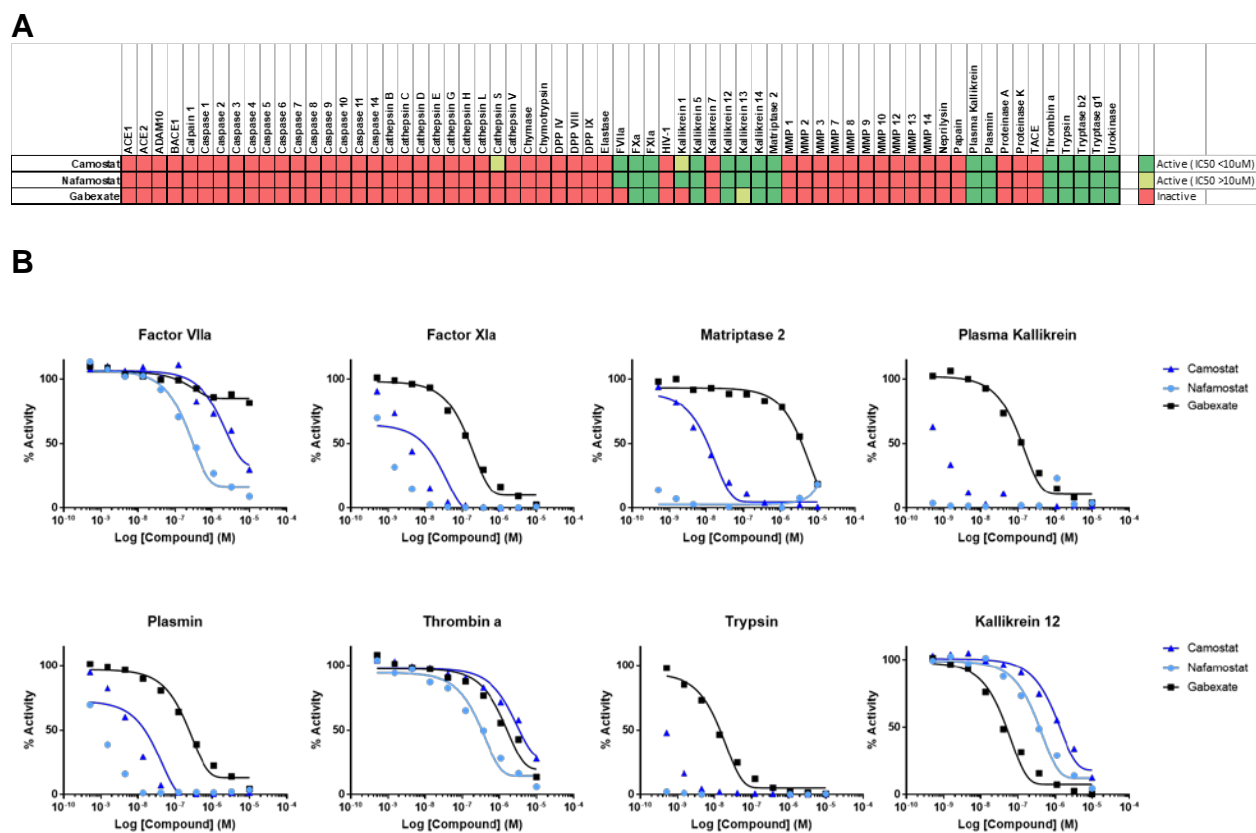


Figure 4: Activity of camostat, nafamostat and gabexate against a panel of proteases. **A)** Compounds were tested against all proteases in dose-response, and activity data was conditionally formatted, dark green = inhibition ($IC_{50} \leq 10\mu M$), light green = ($IC_{50} > 10\mu M$), and red = inactive. **B)** Dose-response curves for all three compounds against the eight most sensitive proteases in the panel (full report in Supplemental RB Report).

References

1. Guy, R. K.; DiPaola, R. S.; Romanelli, F.; Dutch, R. E., Rapid repurposing of drugs for COVID-19. *Science* **2020**, *368* (6493), 829-830.
2. Tu, Y. F.; Chien, C. S.; Yarmishyn, A. A.; Lin, Y. Y.; Luo, Y. H.; Lin, Y. T.; Lai, W. Y.; Yang, D. M.; Chou, S. J.; Yang, Y. P.; Wang, M. L.; Chiou, S. H., A Review of SARS-CoV-2 and the Ongoing Clinical Trials. *Int J Mol Sci* **2020**, *21* (7).
3. Eastman, R. T.; Roth, J. S.; Brimacombe, K. R.; Simeonov, A.; Shen, M.; Patnaik, S.; Hall, M. D., Remdesivir: A Review of Its Discovery and Development Leading to Emergency Use Authorization for Treatment of COVID-19. *ACS Cent Sci* **2020**, *6* (5), 672-683.
4. Strope, J. D.; Pharm, D. C.; Figg, W. D., TMPRSS2: Potential Biomarker for COVID-19 Outcomes. *J Clin Pharmacol* **2020**, *60* (7), 801-807.
5. Kawase, M.; Shirato, K.; van der Hoek, L.; Taguchi, F.; Matsuyama, S., Simultaneous Treatment of Human Bronchial Epithelial Cells with Serine and Cysteine Protease Inhibitors Prevents Severe Acute Respiratory Syndrome Coronavirus Entry. *Journal of Virology* **2012**, *86* (12), 6537-6545.
6. Shirato, K.; Kawase, M.; Matsuyama, S., Middle East respiratory syndrome coronavirus infection mediated by the transmembrane serine protease TMPRSS2. *J Virol* **2013**, *87* (23), 12552-61.
7. Yamamoto, M.; Matsuyama, S.; Li, X.; Takeda, M.; Kawaguchi, Y.; Inoue, J.-i.; Matsuda, Z., Identification of Nafamostat as a Potent Inhibitor of Middle East Respiratory Syndrome Coronavirus S Protein-Mediated Membrane Fusion Using the Split-Protein-Based Cell-Cell Fusion Assay. *Antimicrobial Agents and Chemotherapy* **2016**, *60* (11), 6532-6539.
8. Hoffmann, M.; Kleine-Weber, H.; Schroeder, S.; Krüger, N.; Herrler, T.; Erichsen, S.; Schiergens, T. S.; Herrler, G.; Wu, N.-H.; Nitsche, A.; Müller, M. A.; Drosten, C.; Pöhlmann, S., SARS-CoV-2 Cell Entry Depends on ACE2 and TMPRSS2 and Is Blocked by a Clinically Proven Protease Inhibitor. *Cell* **2020**, *181* (2), 271-280.e8.
9. De Savi, C.; Hughes, D. L.; Kvaerno, L., Quest for a COVID-19 Cure by Repurposing Small-Molecule Drugs: Mechanism of Action, Clinical Development, Synthesis at Scale, and Outlook for Supply. *Organic Process Research & Development* **2020**, *24* (6), 940-976.
10. <https://clinicaltrials.gov/ct2/results?cond=&term=camostat&cntry=&state=&city=&dist=>
11. Fujii, S. U., Y.; Watanabe, T.; Kayama, N. Guanidinobenzoic Acid Derivatives. 1977.
12. Senokuchi, K.; Nakai, H.; Nakayama, Y.; Odagaki, Y.; Sakaki, K.; Kato, M.; Maruyama, T.; Miyazaki, T.; Ito, H.; Kamiyasu, K.; Kim, S.-i.; Kawamura, M.; Hamanaka, N., New Orally Active Serine Protease Inhibitors. *Journal of Medicinal Chemistry* **1995**, *38* (14), 2521-2523.
13. Meyer, D.; Sielaff, F.; Hammami, M.; Böttcher-Friebertshäuser, E.; Garten, W.; Steinmetzer, T., Identification of the first synthetic inhibitors of the type II transmembrane serine protease TMPRSS2 suitable for inhibition of influenza virus activation. *Biochemical Journal* **2013**, *452* (2), 331-343.
14. Lucas, J. M.; Heinlein, C.; Kim, T.; Hernandez, S. A.; Malik, M. S.; True, L. D.; Morrissey, C.; Corey, E.; Montgomery, B.; Mostaghel, E.; Clegg, N.; Coleman, I.; Brown, C. M.; Schneider, E. L.; Craik, C.; Simon, J. A.; Bedalov, A.; Nelson, P. S., The Androgen-Regulated Protease TMPRSS2 Activates a Proteolytic Cascade Involving Components of the Tumor Microenvironment and Promotes Prostate Cancer Metastasis. *Cancer Discovery* **2014**, *4* (11), 1310-1325.
15. Brimacombe, K. R.; Zhao, T.; Eastman, R. T.; Hu, X.; Wang, K.; Backus, M.; Baljinnyam, B.; Chen, C. Z.; Chen, L.; Eicher, T.; Ferrer, M.; Fu, Y.; Gorshkov, K.; Guo, H.; Hanson, Q. M.; Itkin, Z.; Kales, S. C.; Klumpp-Thomas, C.; Lee, E. M.; Michael, S.; Mierzwa, T.; Patt, A.; Pradhan, M.; Renn, A.; Shinn, P.; Shrimp, J. H.; Viraktamath, A.; Wilson, K. M.; Xu, M.; Zakharov, A. V.; Zhu, W.; Zheng, W.;

- Simeonov, A.; Mathé, E. A.; Lo, D. C.; Hall, M. D.; Shen, M., An OpenData portal to share COVID-19 drug repurposing data in real time. *bioRxiv* **2020**.
16. Böttcher-Friebertshäuser, E.; Freuer, C.; Sielaff, F.; Schmidt, S.; Eickmann, M.; Uhlendorff, J.; Steinmetzer, T.; Klenk, H. D.; Garten, W., Cleavage of influenza virus hemagglutinin by airway proteases TMPRSS2 and HAT differs in subcellular localization and susceptibility to protease inhibitors. *J Virol* **2010**, *84* (11), 5605-14.
 17. WILSON, S.; GREER, B.; HOOPER, J.; ZIJLSTRA, A.; WALKER, B.; QUIGLEY, J.; HAWTHORNE, S., The membrane-anchored serine protease, TMPRSS2, activates PAR-2 in prostate cancer cells. *Biochemical Journal* **2005**, *388* (3), 967-972.
 18. Koutsopoulos, S.; Patzsch, K.; Bosker, W. T. E.; Norde, W., Adsorption of Trypsin on Hydrophilic and Hydrophobic Surfaces. *Langmuir* **2007**, *23* (4), 2000-2006.
 19. Hoffmann, M.; Schroeder, S.; Kleine-Weber, H.; Müller, M. A.; Drosten, C.; Pöhlmann, S., Nafamostat Mesylate Blocks Activation of SARS-CoV-2: New Treatment Option for COVID-19. *Antimicrobial Agents and Chemotherapy* **2020**, *64* (6), e00754-20.
 20. Goettig, P.; Brandstetter, H.; Magdolen, V., Surface loops of trypsin-like serine proteases as determinants of function. *Biochimie* **2019**, *166*, 52-76.
 21. Ramsay, A. J.; Hooper, J. D.; Folgueras, A. R.; Velasco, G.; López-Otín, C., Matriptase-2 (TMPRSS6): a proteolytic regulator of iron homeostasis. *Haematologica* **2009**, *94* (6), 840-849.
 22. Dahlbäck, B.; Villoutreix, B. O., Regulation of Blood Coagulation by the Protein C Anticoagulant Pathway. *Arteriosclerosis, Thrombosis, and Vascular Biology* **2005**, *25* (7), 1311-1320.
 23. Maggio, R.; Corsini, G. U., Repurposing the mucolytic cough suppressant and TMPRSS2 protease inhibitor bromhexine for the prevention and management of SARS-CoV-2 infection. *Pharmacol Res* **2020**, *157*, 104837.
 24. Ohno, H.; Kosaki, G.; Kambayashi, J.; Imaoka, S.; Hirata, F., FOY: [Ethylp-(6-guanidinohexanoyloxy) benzoate] methanesulfonate as a serine proteinase inhibitor. I. Inhibition of thrombin and factor Xa in vitro. *Thrombosis Research* **1980**, *19* (4), 579-588.
 25. Asakura, H.; Ogawa, H., Potential of heparin and nafamostat combination therapy for COVID-19. *Journal of Thrombosis and Haemostasis* **2020**, *18* (6), 1521-1522.
 26. McGonagle, D.; O'Donnell, J. S.; Sharif, K.; Emery, P.; Bridgewood, C., Immune mechanisms of pulmonary intravascular coagulopathy in COVID-19 pneumonia. *The Lancet Rheumatology* **2020**.
 27. Tsukagoshi, S., [Pharmacokinetics studies of nafamostat mesilate (FUT), a synthetic protease inhibitor, which has been used for the treatments of DIC and acute pancreatitis, and as an anticoagulant in extracorporeal circulation]. *Gan To Kagaku Ryoho* **2000**, *27* (5), 767-74.
 28. .
 29. Midgley, I.; Hood, A. J.; Proctor, P.; Chasseaud, L. F.; Irons, S. R.; Cheng, K. N.; Brindley, C. J.; Bonn, R., Metabolic fate of ¹⁴C-camostat mesylate in man, rat and dog after intravenous administration. *Xenobiotica* **1994**, *24* (1), 79-92.